Journal of Organometallic Chemistry 744 (2013) 82–91

Contents lists available at SciVerse ScienceDirect

Journal of Organometallic Chemistry

journal homepage: www.elsevier.com/locate/jorganchem

Synthetic strategies for efficient conjugation of organometallic complexes with pendant protein reactive markers

Dominik Jantke [a,2], Alexander N. Marziale [a,2], Thomas Reiner [b,1,2], Florian Kraus [b], Eberhardt Herdtweck [b], Andreas Raba [b], Jörg Eppinger [a,*]

[a] King Abdullah University of Science and Technology, Division for Physical Sciences & Engineering and KAUST Catalysis Center, Thuwal, Saudi Arabia
[b] Department Chemie, Technische Universität München, Lichtenbergstr. 4, D-85747 Garching bei München, Germany

ARTICLE INFO

Article history:
Received 19 March 2013
Received in revised form
14 May 2013
Accepted 15 May 2013

Dedicated to Professor Wolfgang A. Herrmann on the occasion of his 65th birthday.

Keywords:
Bioinorganic chemistry
Metalloenzymes
Peptide coupling
Protease inhibitors

ABSTRACT

Site-directed conjugation of metal centers to proteins is fundamental for biological and bioinorganic applications of transition metals. However, methods for the site-selective introduction of metal centers remain scarce. Herein, we present broadly applicable synthetic strategies for the conjugation of bioactive molecules with a range of organometallic complexes. Following three different synthetic strategies, we were able to synthesize a small library of metal conjugated protein markers featuring different types of protein reactive sites (epoxides, phenylphosphonates, fluorosulfonates and fluorophosphonate groups) as well as different late transition metals (iron, ruthenium, rhodium, palladium and platinum). The products were isolated in moderate to excellent yields and high purity. Furthermore, X-ray diffraction of the metalated protein markers corroborates structural integrity of the metal complex and the protein reactive site.

1. Introduction

The conjugation of artificial metal centers to biologically active organic molecules or biomolecules as well as the study of naturally occurring metal centers in enzymes has been investigated intensively over the last decades [1]. Numerous applications and techniques based on metals in biological systems, both naturally as well as non-naturally occurring, were developed. Of particular interest are applications of metal-containing bioconjugates including pharmaceuticals [2], contrast agents for molecular imaging [3], X-ray fluorescence spectroscopy and microscopy [4], or tools to study metalloprotein structure and function [5]. For analytical techniques, artificially incorporated non-naturally occurring metal centers feature the important advantage of providing high signal to noise ratios, since the only source of signal is the artificially introduced metal [6]. Exchange of a protein's naturally occurring catalytically active metal center allowed to alter its electrochemical potential [7], facilitating the use of such systems for the generation of electrochemical biosensors [8]. Research in the flourishing field of artificial metalloenzymes has provided access to a wide range of biocatalytic transformations which do not occur in nature [9]. Wilson and Whitesides introduced site directed anchoring of artificial cofactors based on the biotin–(strept)avidin technology to incorporate artificial metal centers through a supramolecular assembly process [10]. Using directed evolution, Ward and coworkers were able to reveal the full potential of this approach and develop highly enantioselective organometallic enzyme hybrid (OMEH) catalysts for hydrogenations and transfer hydrogenations [11], asymmetric Pd-catalyzed allylations [12], cis-dihydroxylation of olefins [13] and olefin metathesis [14] of transition metal bearing biomolecules. Recently, even catalytic cascade reactions [15] and protein-accelerated asymmetric C–H activations [16] were reported. Covalent attachment of artificial organometallic cofactors has been applied to convert proteases [17], lipases [18] or other non-metal proteins [19] into OMEH catalysts. Expanding this approach, we were recently able to introduce a building block based strategy to generate artificial enantioselective hydrogenases [20]. This approach provides a site-selective, covalent modification method for of a variety of biomolecules with libraries of organometallic complexes via reactive epoxide peptidomimetics.

Despite the plethora of methods and practical applications relying on conjugates of organometallic complexes with biologically active

* Corresponding author. Tel.: +996 2 808 2414.
E-mail address: jorg.eppinger@kaust.edu.sa (J. Eppinger).
[1] Present address: Department of Radiology, Memorial Sloan-Kettering Cancer Center, 1275 York Avenue, New York, NY 10065, USA.
[2] These authors contributed equally.

0022-328X/$ – see front matter © 2013 Elsevier B.V. All rights reserved.
http://dx.doi.org/10.1016/j.jorganchem.2013.05.027

molecules, laborious synthetic access to these compounds is a major limitation. Commonly biomolecular components tend to coordinate the metal center, which hampers conjugation yields. A variety of bioorthogonal conjugation methods have been developed [21], however, the synthesis of orthogonal reactive moieties can be tedious and low-yielding. We therefore decided to systematically study methods, which could enable the conjugation of a range of transition metal complexes via conventional amide linkage. This approach has the advantage, that the required amine and carboxylic functional groups can be introduced easily during complex or biomarker synthesis. The present study describes three different general protocols that permit direct attachment of organometallic complexes to epoxide, diphenylphosphonate, fluorophosphonate and fluorosulfonate protease inhibitors. Each protocol is particularly mild and facilitates conjugation of the metal complex and the reactive functional group without compromising the integrity of the metal center's inner coordination sphere or the reactive functionality of the biomarker moiety.

2. Results and discussion

2.1. Synthesis of transition metal complexes and bioactive marker moieties

Conjugation of metal complexes and bioactive markers via amide linkage requires the presence of an amine function in either of the two building blocks. The nucleophilic NH-moiety can react with the reactive group of the type of protease labels we intended to use in this study. Correspondingly, organometallic complexes were synthesized with a pendant primary or secondary amine group, while the bioactive moieties display a carboxylic acid functional handle. Six amino-functionalized organometallic complexes served as model complexes to test their conjugation with carboxylic acids under amide bond forming conditions (Fig. 1). These complexes represent three different classes:

(i) Amine functionalized half sandwich complexes, which may provide ligand coordination sites following dissociation of the kinetically labile halide–metal bonds (η^5-tetramethyl cyclopentadienyl rhodium **1** [22], and η^6-benzene ruthenium **2** [23]); these complexes are highly stable toward air and moisture and are active catalysts for the hydrogenation of alkenes and ketones in aqueous solution.
(ii) Amine functionalized sandwich complexes, which could serve as redox-active probes for protein detection aminomethylene ferrocene **3** [1,24].
(iii) Transition metal complexes with chelating phosphine ligands represented by complexes **4**, **5** and **6**. These complexes are derived from the chelating bis-phosphine ligands $HN(CH_2CH_2P^iPr_2)_2$ (PNP) and (*R*,*R*)-pyrphos. Palladium complexes coordinated to PNP ligands have been synthesized before [25] and were successfully applied as asymmetric allylic amination catalysts. Late transition metal complexes of (*R*,*R*)-pyrphos have been used for both, immobilization on polymers as well as the generation of dendrimeric catalysts [26]. The corresponding platinum complex **6** of (*R*,*R*)-pyrphos may serve as a ^{195}Pt NMR probe and enable active monitoring in biological systems [27].

All complexes were synthesized as reported previously and characterized by ^{1}H and ^{13}C NMR spectroscopy as well as elemental analysis.

A large number of small organic molecules and peptidomimetics which bear reactive functional groups capable of covalently inhibiting enzymes have been described in literature [28]. Here, we focus on the carboxylic acid forms of established cysteine and serine protease inhibitors (Fig. 2). E64 analog **7** [29], exhibits high binding affinity over a broad group of cysteine proteases of the papain family. The inhibition proceeds via a nucleophilic attack at the inhibitor's epoxide moiety and results in formation of a covalent link between protease and inhibitor. Serine protease reactive markers derived from electrophilic phosphorous and sulfur centers were also used in this study. Diphenylphosphonate **8**, fluorosulfonate **9** and fluorophosphonate **10** [30] are known to bind irreversibly to serine hydrolases. Inhibitors **7** and **10** were synthesized according to literature procedures in high purity and yields. Phosphonate **8** was synthesized by conversion of diphenyl 1-aminobenzyl phosphonate [31] with succinic anhydride. Fluorosulfonate **9** is commercially available and was used as received. All protease inhibitors were characterized by ^{1}H and ^{13}C NMR spectroscopy.

Standard amide bond formation procedures involve conversion of the carboxylic acid into an active ester or anhydride, which can undergo nucleophilic attack by primary or secondary amines. We investigated three general strategies for conjugation of the metal complex with the bioactive marker moiety: (A) post-metal-coordination conjugation, which represent the only possible method for (half)sandwich complexes; (B) pre-metal conjugation, which is an additional option for chelating diphosphines; (C) conjugation via reactive fluorine species, which is a variant of the post-metal-coordination conjugation approach for inhibitors **8**–**10** with electrophilic phosphorus and sulfur centers.

2.1.1. Method *A*: post-coordination conjugation

In order to establish a general synthetic route for the attachment of metal complexes to protein reactive markers via post-coordination conjugation, we decided to use the air and moisture

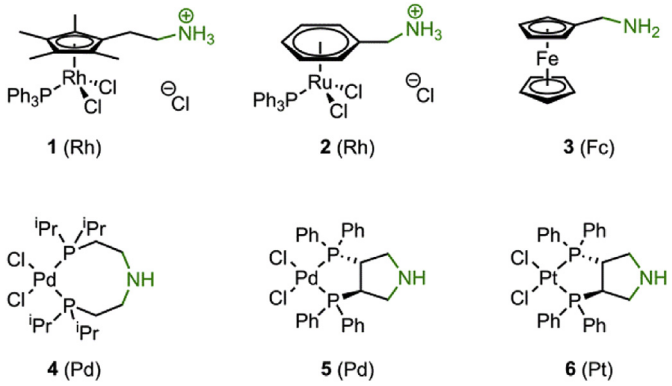

Fig. 1. Metal complexes exhibiting non-coordinating amine groups used in this study.

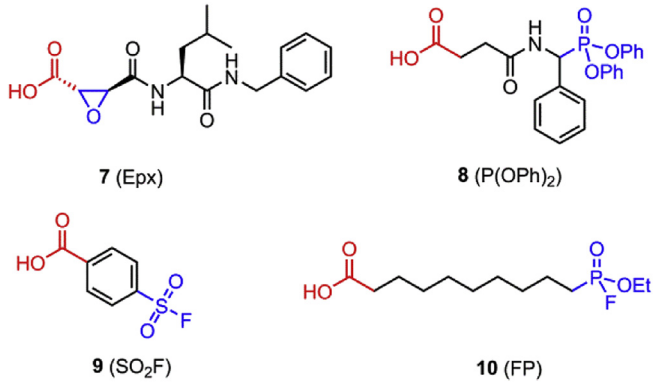

Fig. 2. Organic precursors used for the generation of metalated protein markers.

Table 1
Crystallographic data for **11**.

Formula	$C_{46}H_{53}Cl_2N_3O_4PRh$
Formula wt	916.69
Space group	$P2_1$
a (Å)	8.7620(3)
b (Å)	32.5384(10)
c (Å)	8.8665(3)
α (°)	90
β (°)	109.700(2)
γ (°)	90
V (Å^3)	2379.9(1)
Z	2
$D_{calc.}$ (g cm^{-3})	1.279
No. of indep rflns	10,172
No. of params	500
$R1$ ($I > 2\sigma(I)$)	0.047
$wR2$ (all data)	0.122
Goodness of fit	1.237
Flack x	0.05(3)

stable rhodium complex **1** and protein marker **7** as test system. During the initial condition screen we found that typical peptide coupling reagents such as dicyclohexyl carbodiimide, *N*-hydroxy succinimide or substituted benzotriazoles tend to coordinate to the metal center and alter the inner coordination sphere of the catalyst. However, activation of the carboxylic acid with a polystyrene bound solid phase cyclohexyl carbodiimide derivative followed by conversion of the intermediate with an excess of pentafluorophenol circumvents this problem. The resulting activated pentafluorophenol esters can easily be conjugated with amines. Filtration of the carbodiimide resin before addition of complex **1** ensures that its nucleophilic centers (e.g. urea based side products) do not lead to side product formation. More importantly, pentafluorophenol exhibits negligible binding affinity for the ruthenium(II) center, leaving the inner coordination sphere of the metal complex unaltered. Coupling via pentafluorophenol ester intermediates yielded the rhodium containing protein marker **11** in 86% and the ruthenium compound **12** in 68% yield (see Table 3). Purity, stability and identity of both complexes complex were confirmed by ^{1}H, ^{13}C, ^{31}P NMR and ^{1}H^{1}H COSY NMR spectroscopy, IR spectroscopy, elemental analysis and mass spectrometry. ^{31}P NMR spectra display the characteristic signals for the coordinated phosphine ligand (**11**: doublet, $\delta = 30.0$ ppm, $^1J_{Rh,P} = 143$ Hz; **12**: singlet, $\delta = 27.8$ ppm), which are in agreement with literature values of similar compounds [22,23,32]. This proves that the metal coordination environment was not changed during the conjugation process. The ^{1}H and ^{13}C NMR spectra of the epoxide moiety closely resemble those of the E64 derived precursor. Hence it can be concluded, that the epoxide moiety is still intact. The NH protons of the pendant linker resonate at 7.97 ppm (**11**) and approx. 7.0 ppm (**12**, overlay with arene protons), which underlines that conjugation via amide linkage was successful. Only one set of signals is observed for both protein markers. The inhibitor moiety has three stereocenters, and racemization of one of them would lead to formation of diastereomers with distinguishable spin systems. Therefore the stereochemistry is confirmed to be unaltered.

Table 2
Crystallographic data for **17**.

Formula	$2(C_{36}H_{36}Cl_2FNO_3PRhS)$, $3(CHCl_3)$
Formula wt	1931.12
Space group	P-1 (no. 2)
a (Å)	15.0745(9)
b (Å)	16.9192(10)
c (Å)	18.5003(12)
α (°)	69.352(3)
β (°)	73.986(4)
γ (°)	69.983(3)
V (Å^3)	4083.5(4)
Z	2
$D_{calc.}$(g cm^{-3})	1.571
No. of indep rflns	11,695
No. of params	945
$R1$ ($I > 2\sigma(I)$)	0.0410
$wR2$ (all data)	0.1146
Goodness of fit	1.046
Largest diff. peak and hole (e Å^{-3})	1.06/−0.77

Crystals of complex **11** suitable for X-ray crystallographic analysis were obtained from a 0.02 M solution in methanol at −18 °C. The structure of this complex, which crystallizes in the monoclinic space group $P2_1$ is shown in Fig. 2, crystallographic parameters are found in Tables 1 and 2. The crystal structure confirms the integrity of the piano-stool shaped rhodium complex. All bond length and angles are within the expected range [33]. The distances of the protein reactive epoxide carbon atoms from the rhodium center are 8.006(6) Å and 9.063(6) Å respectively. No intra- or inter-molecular interactions between the metal center and the epoxide or the amide bonds are found in the crystal. The high flexibility of the terminal benzyl group and the leucine side chain is attributed to very weak H-bond interactions in the crystal. The Flack parameter $x = 0.05(3)$ confirms retention of the stereochemistry of the epoxide as well as the amino acid side chain. The linear structure illustrates of how this artificial metallo-cofactor should bind to a protease: the inhibitor moiety maps the hydrophilic binding pockets, while the epoxide moiety forms the covalent link at the active center. This double interaction orients the cofactor in the binding pocket of the protease. Structural flexibility is only expected to arise from the ethylene linker between the metal complex and the E64 inhibitor moiety (Fig. 3).

Method **A** is also suitable for the metal complex conjugation of bioactive molecules comprising electrophilic heteroatoms. The bioactive metalated marker **15** was obtained from rhodium complex **1** and phosphonate **8** in 68% yield. Purity, stability and identity of the rhodium conjugated marker were confirmed by homo- and hetero-nuclear NMR spectroscopy, IR spectroscopy, elemental analysis and mass spectrometry. ^{31}P NMR spectroscopy shows the expected doublet for the triphenylphosphine ligand at $\delta = 29.8$ ppm with the typical coupling constant of $^1J_{Rh,P} = 143$ Hz and a singlet at $\delta = 14.8$ ppm for the phosphonate.

Fluorosulfonates are well established efficient inhibitors of serine proteases. We decided to use the commercially available fluorosulfonate **3** in our study since it exhibits a carboxylic acid functional handle. Conjugation with ruthenium complex **1** and ferrocene derivative **3** by the *post-coordination conjugation* method yields metalated protein marker **18** and **19** in high purity and moderate yields (**18**: 43% **19**: 20%). Stability of the fluorosulfonate is confirmed by ^{19}F NMR spectroscopy, showing clean singlets at 66.28 ppm (**18**) and 66.08 ppm (**19**). Structural integrity of the metal complexes moiety of **18** is evident form NMR spectroscopy. In the ^{31}P NMR, a singlet is observed for the metal bound triphenylphosphine at $\delta = 28.0$ ppm. The ferrocene-conjugated marker shows the characteristic signals of the Cp-protons as well as the NH resonance at 6.38 ppm.

2.1.2. Method *B*: pre-coordination conjugation

The secondary amine functions of complexes **4**–**6** provide only reduced reactivity and therefore require longer reaction times. Correspondingly, method **A** provides only low yields and impure products for conversions of the PNP–palladium complex **4** with phenylphosphonate **8**. Both, the loss of the metal center as well as decomposition of the reactive phosphonate moiety are responsible for the unsatisfactory conjugation results. Hence, for the bisphosphine complexes of palladium and platinum we decided to test

Table 3
Schematic representation of the different synthetic strategies used for the generation of metalated protein markers.

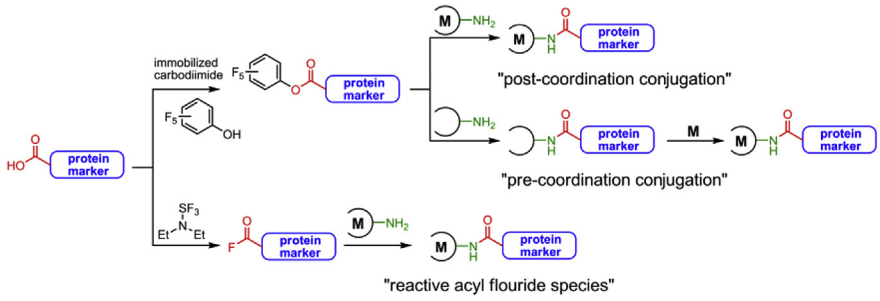

Compound	Structure	Method, yield	Reactive moiety	Protease family
11	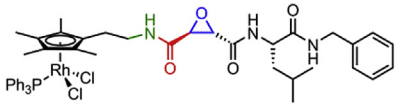	**A**, 86%	Epoxide	Cysteine proteases
12	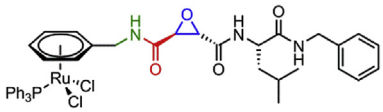	**A**, 79%	Epoxide	Cysteine proteases
13	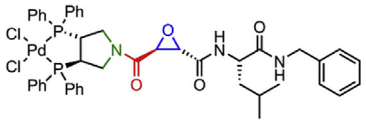	**A**, 89% **B**, 92%	Epoxide	Cysteine proteases
14	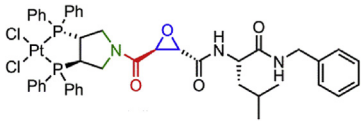	**A**, 87% **B**, 95%	Epoxide	Cysteine proteases
15	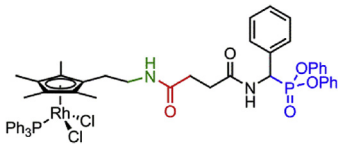	**A**, 68%	Diphenyl-phosphonate	Serine proteases
16	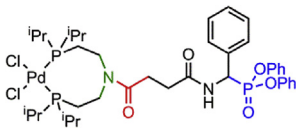	**B**, 89%	Diphenyl-phosphonate	Serine proteases
17	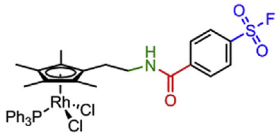	**A**, 59% **C**, 95%	Fluorosulfonate	Serine proteases
18	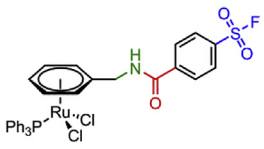	**A**, 43% **C**, 89%	Fluorosulfonate	Serine proteases
19	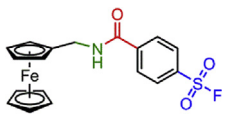	**A**, 20%	Fluorosulfonate	Serine proteases
20	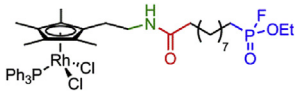	**C**, 86%	Fluoro-phosphonate	Serine proteases

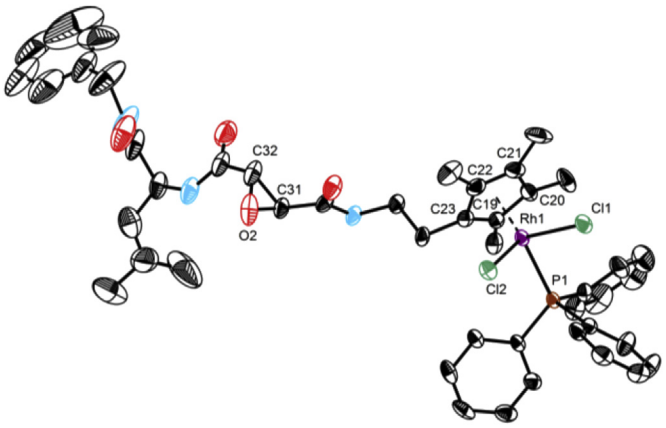

Fig. 3. Crystal structure of rhodium functionalized protein marker **11**. Hydrogen atoms are omitted for clarity. Thermal ellipsoids are shown at a 30% probability level.

conjugation of ligands and reactive organic molecules prior to coordination of the transition metal centers. This *pre-coordination conjugation* approach allowed the straightforward synthesis of ligand functionalized protein reactive markers, which are readily converted metal-conjugated affinity markers upon addition of the transition metal precursor. Following formation of the pentafluorophenol ester, phenylphosphonate **8** was functionalized with the PNP-ligand. Stirring with $PdCl_2(CH_3CN)_2$ converted the active ester into the metalated protein marker **16**, which was isolated in high yield (89%). Excellent purity and structural integrity were confirmed by NMR spectroscopy, elemental analysis, IR spectroscopy and mass spectrometry. The free ligand is air and moisture sensitive, however after palladium-coordination and *N*-functionalization it displays excellent stability toward air and moisture.

Activation of the carboxylic acid of **7** by immobilized cyclohexyl carbodiimide and formation of the pentafluorophenol active ester followed by addition of the non-metalated ligand (*R*,*R*)-pyrphos, resulted in clean formation of the peptide bond between the protein marker and the ligand. Subsequent attachment of the metal center was achieved by addition of the metal precursors $PdCl_2(CH_3CN)_2$ or $PtCl_2(CH_3CN)_2$, yielding complexes **13** and **14**, respectively. Clean product formation was observed in both cases. The metalated protein markers are highly stable toward air and moisture. Both complexes **13** and **14** are stable on silica columns, which allowed their purification by column chromatography yielding the protein markers in 92% and 95% isolated yield (**13** and **14**, respectively). For the active ester of inhibitor **7**, coupling was also successful when metal complexes **5** and **6** were used directly, however this resulted in slightly lower yields (89% and 87% for **13** and **14**, respectively).

2.1.3. Method **C**: reactive acyl fluoride species

Synthesis of transition metal centers covalently linked to the serine hydrolase inhibitors fluorophosphonate **9** or fluorosulfonate **10** was realized following a different strategy. The corresponding precursors **9** and **10** were treated with diethylamino sulfurtrifluoride (DAST), resulting in the generation of acyl fluorides, a technique described by Liu et al. [30] Acyl fluorides exhibit high reactivity toward nucleophiles but posses only limited affinity toward transition metal complexes, rendering the possibility to use these reactive fluoride species directly for the formation of metal-conjugated protease markers **17** and **20**. The fluorosulfonate marker **17** was isolated in 95% yield. Following the *post-coordination conjugation* approach, the same complex was isolated in 59% yield, showing the advantages of the reactive acyl fluoride reaction sequence. The product was characterized using homo- and heteronuclear NMR spectroscopy, ESI-MS and elemental analysis. In ^{19}F NMR spectroscopy, only one singlet was observed, which was assigned to the fluorosulfonic acid fluoride (85.86 ppm). Furthermore, in ^{31}P NMR, the doublet originating from the triphenylphosphine phosphorous is indicative for the success of the reaction. It was observed at 30.04 ppm ($^1J_{Rh,P} = 143$ Hz). In ^1H NMR, a triplet originating from the peptide NH proton was observed at 8.12 ppm with a coupling constant of $^3J_{HH} = 5.8$ Hz.

Crystals suitable for X-ray analysis of complex **17** were obtained from a mixture of $CH_2Cl_2/Et_2O/CHCl_3/CDCl_3$ at −18 °C at a concentration of approx. 40 mg/mL. The structure, which was solved in the space group P-1 shows integrity of the metal centers inner coordination sphere with no intra- or inter-molecular interactions between the metal center and the outer ligand sphere as well as stability of the fluorosulfonate moiety toward synthetic and crystallographic methods (Fig. 4). In the unit cell, two non-equivalent molecules of **17** are present, which only show small differences in bond lengths and angles. The Rh center, which is in a slightly distorted piano-stool geometry, shows no unexpected distortions. Angles between Rh and the ligands are in the expected range. The bond length between Rh and Cp* centroid with 1.824(2) and 1.821(2) Å are in the range of similar Rh–Cp* complexes. This is expected due to the similar steric demand of the methyl group and the pendant linker group of the Cp* ring system. Also Rh–Cl bond lengths are very similar, ranging from 2.3858(12) to 2.4258(11) Å. The Cl1–Rh1–Cl2 angle (91.36(4)°) is only slightly larger than the two P1–Rh1–Cl angles (87.74(5)° and 86.92(4)°). The F–S–O angles of both independent molecules in the unit cell are (105.2(2)°, 104.9(2)° and 106.4(3)° 111.7(3)°).

The metal-conjugated biomarkers **18** and **20** were obtained by addition of the respective metal complexes (Ru complex **2** for **18** and Rh complex **1** for **20**) to the crude acyl fluoride of the reactive biomarker moiety (epoxide **7** for **18** and fluorophosphonate **10** for **20**) in presence of NEt_3. The analytically pure product was isolated in 89% and 86% yield after aqueous workup and etheric precipitation from a dichloromethane solution. Compound **18** gave signals identical to those of the compound which was synthesized by the post-coordination conjugation method. Structural identity of the fluorophosphonate functionality in **20** and the metal center's integrity as well as purity of the product was confirmed by homo- and hetero-nuclear NMR spectroscopy, IR spectroscopy, elemental analysis and mass spectrometry. ^{31}P NMR shows a characteristic doublet at $\delta = 29.8$ ppm with $^1J_{Rh,P} = 142$ Hz and a doublet at $\delta = 32.5$ ppm with $^1J_{F,P} = 1.07$ kHz.

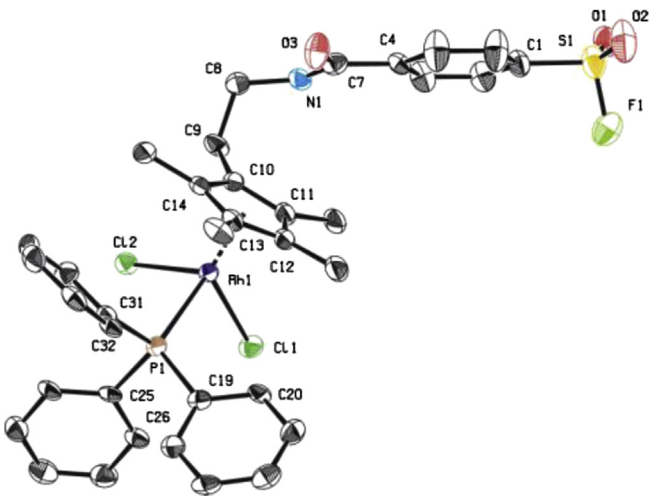

Fig. 4. ORTEP representation of one molecule in the unit cell of **17**. Hydrogen atoms are omitted for clarity. Thermal ellipsoids are shown at the 50% probability level.

3. Conclusion

Our studies revealed that post-metal-coordination assembly method **A** is suitable for amide bond formation for all three types of metal complexes tested in this study. The successful strategy is based on utilization of solid phase coupling reagents to form an active pentafluorophenyl ester intermediate. While method **A** can be applied for a broad range of compounds, pre-metal-coordination assembly (method **B**) and conjugation via active acid fluorides (method **C**) leads to higher yields for chelating diphosphines (**B**) and inhibitors with electrophilic phosphorous and sulfur centers (**C**). Our synthetic strategy enabled us to synthesize and characterize a broad range of Fe, Ru, Rh, Pd and Pt containing biomarkers including several, which provide a catalytically active transition metal center. The particularly mild coupling procedures leave the protein reactive group as well as the organometallic moiety unaltered, which was confirmed by spectroscopic data and X-ray crystallography of two metalated protein markers. All compounds presented in this study are stable against air and moisture, which makes them promising candidates for further applications directed toward molecular imaging or generation of catalytically active organometallic enzyme hybrids. The approach can be further used to generate libraries of metal containing bioactive molecules, which should facilitate optimization and application of such compounds.

4. Experimental section

4.1. General methods

All reactions involving air-sensitive compounds were performed under an atmosphere of argon using standard Schlenk and glove-box techniques. THF was dried over Na/benzophenone, distilled under argon and deoxygenated prior to use. Diethyl ether, pentane and hexane were dried and deoxygenized by passing through columns packed with activated alumina and Q5, respectively. Dichloromethane was dried over CaH_2 and distilled prior to use. $CDCl_3$ was dried over CaH_2 and purified by condensation and deoxygenated by three *freeze–pump–thaw* cycles. NMR spectra were recorded on a JEOL JNM-GX 400, a BRUKER DRX 400, a Bruker Avance III 400 and a Bruker Avance III 500. Chemical shifts are given in ppm and were referenced to the residual proton resonance respectively the natural abundance ^{13}C resonance of the solvent. ^{31}P NMR spectra were calibrated to an external standard (phosphoric acid). ESI-MS and ESI-LC MS spectra were recorded on a LCQ classic spectrometer (Thermo Electron). Elemental analyses were obtained from the Microanalytical Laboratory of Technische Universität München. IR spectra were recorded on a Jasco FT/IR-460 PLUS and prepared as KBr pallets or Nujol suspension between KBr plates. Wavelengths are noted in cm^{-1}. Data were collected on an X-ray single crystal diffractometer equipped with a CCD detector (Bruker APEX II, κ-CCD), a rotating anode (Bruker AXS, FR591) with MoK_α radiation (λ = 0.71073 Å), and a graphite monochromator by using the SMART software package [34]. The measurements were performed on a single crystal coated with perfluorinated ether. The crystal was fixed on the top of a glass fiber and transferred to the diffractometer. The crystal was frozen under a stream of cold nitrogen at 123 K (**17**) or was measured at 296 K (**11**). A matrix scan was used to determine the initial lattice parameters. Reflections were merged and corrected for Lorenz and polarization effects, scan speed, and background using SAINT [35]. Absorption corrections, including odd and even ordered spherical harmonics were performed using SADABS [35]. Space group assignments were based upon systematic absences, *E* statistics, and successful refinement of the structures. Structures were solved by direct methods with the aid of successive difference Fourier maps, and were refined against all data using WinGX [40] based on SIR-92 [36]. If not mentioned otherwise, non-hydrogen atoms were refined with anisotropic displacement parameters. Methyl hydrogen atoms were refined as part of rigid rotating groups, with C–H = 0.98 Å and $U_{iso(H)} = 1.5U_{eq(C)}$. All other hydrogen atoms were placed in calculated positions and refined using a riding model, with methyne, methylene and aromatic C–H distances of 1.00, 0.99 and 0.95 Å, respectively, and $U_{iso(H)} = 1.2U_{eq(C)}$. N–H distances were set to 0.88 Å and $U_{iso(H)} = 1.2U_{eq(N)}$. Full-matrix least-squares refinements were carried out by minimizing $\sum w(F_o^2 - F_c^2)2$ with SHELXL-97 [38] weighting scheme. Neutral atom scattering factors for all atoms and anomalous dispersion corrections for the non-hydrogen atoms were taken from *International Tables for Crystallography* [37]. Images of the crystal structures were generated by PLATON [39]. Compounds **1** [22], **2** [23], **3** [24], **4** [25], **5** [26], **6** [26], **7** [30] and **10** [31] were synthesized according to literature procedures, compound **9** was purchased from Aldrich and used without any further purification.

4.2. Synthetic procedures

4.2.1. Synthesis of protein marker *8*

Succinic anhydride (354 mg, 3.54 mmol) and diphenyl 1-aminobenzyl phosphonate (1.00 g, 2.95 mmol) were dissolved in dichloromethane (75 mL). Then, pyridine (237 μL, 2.95 mmol) was added and the reaction mixture stirred for 24 h. Thereafter, the mixture was washed with water (3 × 40 mL) and brine (2 × 40 mL), dried over $MgSO_4$ and volatiles removed under reduced pressure. The raw product was redissolved in EtOAc and precipitated with diethyl ether to give the pure product (1.06 g, 2.41 mmol, 68%) as a white solid. ^1H NMR (400 MHz, $CDCl_3$, 25 °C): δ = 8.36 (dd, $^3J_{(H,P)}$ = 13 Hz, $^3J_{(H,H)}$ = 9.6 Hz, 1H, N*H*), 7.54–6.63 (m, 15H, $H_{aromat.}$), 5.96 (dd, $^3J_{(H,H)}$ = 9.6 Hz, $^2J_{(H,P)}$ = 22 Hz, 2H, NHC*H*Ph), 2.64–2.39 (m, 4H, CH_2CH_2COOH); ^{13}C NMR (101 MHz, $CDCl_3$, 25 °C): δ = 176.3 (s, *C*OOH), 171.8 (d, $^3J_{(P,C)}$ = 9.2 Hz, NHCO), 150.3 (d, $J_{(P,C)}$ = 9.9 Hz, $C_{aromat.}$), 150.1 (d, $J_{(P,C)}$ = 11 Hz, $C_{aromat.}$), 133.8 (s, $C_{aromat.}$), 130.0 (d, $J_{(P,C)}$ = 27 Hz, $C_{aromat.}$), 129.4–128.4 (m, 2 $C_{aromat.}$), 125.6 (d, $J_{(P,C)}$ = 24 Hz, $C_{aromat.}$), 120.6 (d, $J_{(P,C)}$ = 3.8 Hz, $C_{aromat.}$), 120.2 (d, $J_{(P,C)}$ = 3.8 Hz, $C_{aromat.}$), 50.7 (d, $^1J_{(P,C)}$ = 159 Hz, PhCH), 30.5 (s, *C*H_2CH$_2$), 29.4 (s, CH$_2$*C*H$_2$); ^{31}P NMR (162 MHz, 25 °C, CDCl3): δ = 15.1; IR (KBr): $\tilde{\nu}$ = 3261 m, 3060 m, 2917 w, 1719 m, 1701 sh w, 1677 m, 1653 s, 1589 m, 1550 m, 1492 s, 1202 m, 1179 m, 942 vs cm^{-1}; MS (ESI): *m*/*z* (%): = 462.2 $[M + Na]^+$, 901.1 $[2M + Na]^+$, 917.1 $[2M + K]^+$;elemental analysis calcd. (%) for $C_{23}H_{22}NO_6P \cdot 0.5H_2O$: C 61.61, H 5.17, N 3.12; found C 62.46, H 4.95, N 3.04.

4.2.2. General coupling procedure A (post-coordination conjugation)

Dichloromethane (10 mL) was added to polystyrene bound cyclohexyl carbodiimide (130 mg, 2.3 mmol/g, 0.30 mmol, 1.5 eq.) at 0 °C and the resin was allowed to swell for 45 min. The corresponding inhibitor (0.20 mmol, 1.0 eq.) and pentafluorophenol (0.30 mmol, 1.5 eq.) were added and the reaction mixture was stirred at 0 °C for 1 h. The reaction was allowed to warm to r.t. and was stirred over night. The mixture was filtered, triethylamine (55 μL, 0.40 mmol, 2.0 eq.) and metal complex (0.20 mmol, 1.0 eq.) were added. The reaction was stirred at r.t. for 3 h. Upon completion, the organic phase was washed with water and brine (each 3 × 10 mL), dried over $MgSO_4$ and volatiles were removed under reduced pressure. The resulting solid was washed with diethyl ether and hexanes to give the pure product.

4.2.3. General coupling procedure B (pre-coordination conjugation)

Dichloromethane (10 mL) was added to polystyrene bound cyclohexyl carbodiimide (130 mg, 2.3 mmol/g, 0.30 mmol, 1.5 eq.) at 0 °C and the resin was allowed to swell for 45 min. The

corresponding inhibitor (0.20 mmol, 1.0 eq.) and pentafluorophenol (0.30 mmol, 1.5 eq.) were added and the reaction mixture was stirred at 0 °C for 1 h. The reaction was allowed to warm to r.t. and was stirred over night. The mixture was filtered, triethylamine (55 μL, 0.40 mmol, 2.0 eq.) and the diphosphine ligand (0.20 mmol, 1.0 eq.) were added. The reaction was stirred at r.t. over night. Volatiles were removed under reduced pressure and the resulting residue was dissolved in dry THF. The solution was filtered and a suspension of the metal precursor (0.19 mmol, 0.95 eq.) in THF (5 mL) was added to the filtrate and the reaction was stirred at r. t. over night. Upon completion of the reaction, diethyl ether (10 mL) and pentane (5 mL) were added and a yellow solid was precipitated. The solid was filtered off and washed with diethyl ether (3 × 15 mL) and volatiles removed *in vacuo*. Subsequently, the product was purified by column chromatography (CH_2Cl_2/MeOH = 95/5) and from the combined product fractions a yellow solid was precipitated by addition of diethyl ether and pentane. The solid was washed with diethyl ether (2 × 15 mL).

4.2.4. General coupling procedure C (reactive acid fluoride species)

The corresponding inhibitor (0.26 mmol, 1.0 eq.) was dissolved in a Teflon-flask in dichloromethane (5 mL) at −78 °C. To this solution, DAST was added (135 μL, 1.02 mmol, 4.0 eq.) and the solution was stirred at −78 °C for 15 min. And was allowed to warm to r.t. Water (10 mL) was added in small portions and the solution was vigorously stirred for 5 min before ethyl acetate (30 mL) was added. The organic phase was separated and washed with brine, dried over $MgSO_4$ and volatiles were removed under reduced pressure. The residual oily substance was dissolved in dichloromethane (5 mL) before triethylamine (143 μL, 1.02 mmol, 4.0 eq.) and the metal complex (0.25 mmol, 0.95 eq.) was added. The reaction solution was stirred at r.t. for 3 h before volatiles were removed *in vacuo*. The resulting solid was dissolved in dichloromethane (3 mL) and the product precipitated by addition hexane (50 mL) at −20 °C over night. The supernatant was filtered off and the red precipitate was washed with hexane and volatiles removed *in vacuo*.

4.2.5. Characterization of metalated protein markers

4.2.5.1. [(η^5-Me$_4$Cp(CH$_2$)$_2$NH-Eps-Leu-Bz)RhCl$_2$(PPh$_3$)] ***11***. This compound was synthesized following general procedure A. The product was obtained as a bright red solid (119 mg, 0.13 mmol, 86%). ^{1}H NMR (400 MHz, $CDCl_3$, 25 °C): δ = 7.82–7.72 (m, 6H, C$H_{aromat.}$), 7.50–7.17 (m, 15H, C$H_{aromat.}$, CH_2CH_2NH), 7.09–6.95 (m, 2H, NH$CH_2(C_6H_5)$, NH*C*H), 4.48–4.40 (m, 1H, NHC*H*), 4.35 (dd, $^2J_{(H,H)}$ = 14.9 Hz, $^3J_{(H,H)}$ = 5.8 Hz, 1H, NHC$H_2(C_6H_5)$), 4.27 (dd, $^2J_{(H,H)}$ = 14.9 Hz, $^3J_{(H,H)}$ = 5.8 Hz, 1H, NHC$H_2(C_6H_5)$), 3.55 (d, $^3J_{(H,H)}$ = 1.9 Hz, 1H, C*H*OCH), 3.53 (d, $^3J_{(H,H)}$ = 1.9 Hz, 1H, CHOC*H*), 3.38 (m, 2H, CH_2CH_2NH), 2.26 (m, 2H, CH_2CH_2NH), 1.69–1.50 (m, 3H, $CH_2CH(CH_3)_2$), 1.49 (d, $^4J_{(P,H)}$ = 2.9 Hz, 3H, $C_{Cp}CH_3$), 1.48 (d, $^4J_{(P,H)}$ = 3.1 Hz, 3H, $C_{Cp}CH_3$), 1.09 (d, $^4J_{(P,H)}$ = 2.9 Hz, 3H, $C_{Cp}CH_3$), 0.99 (d, $^4J_{(P,H)}$ = 2.9 Hz, 3H, $C_{Cp}CH_3$), 0.83 (d, $^3J_{(H,H)}$ = 3.1 Hz, 3H, $CH_2CH(CH_3)_2$), 0.81 (d, $^3J_{(H,H)}$ = 3.1 Hz, 3H, $CH_2CH(CH_3)_2$); ^{13}C NMR (101 MHz, $CDCl_3$, 25 °C): δ = 171.5 (*C*ON), 166.5 (*C*ON), 166.2 (*C*ON), 138.2 ($C_{aromat.}$), 134.8 (d, $^3J_{(P,C)}$ = 9.7 Hz, $C_{aromat.}$), 130.7($C_{aromat.}$), 128.7 ($C_{aromat.}$), 128.1 ($C_{aromat.}$), 127.7 ($C_{aromat.}$), 127.4 ($C_{aromat.}$), 102.5 (d, $^1J_{(Rh,C)}$ = 5.5 Hz, $C_{aromat.}$), 102.3 (d, $^2J_{(Rh,C)}$ = 4.3 Hz, $C_{Cp.}$), 100.3 (dd, $^2J_{(Rh,C)}$ = 6.6 Hz, $^3J_{(P,C)}$ = 6.6 Hz, $C_{Cp.}$), 97.1 (m, C_{Cp}), 54.5 (*C*H(O)CH), 54.1 (CH(O)*C*H), 51.8 (*C*HCH$_2$), 43.5 (NHCH_2), 41.0 (CHCH_2), 36.3 (d, $^4J_{(P,C)}$ = 4.3 Hz, CH_2CH_2NH), 24.8 (*C*H(CH$_3$)$_2$), 24.6 (CH_2CH_2NH), 23.0 (CH(*C*H$_3$)$_2$), 22.1 (CH(*C*H$_3$)$_2$), 9.5 ($C_{Cp.}CH_3$), 8.7 (s, $C_{Cp.}CH_3$); ^{31}P NMR (162 MHz, $CDCl_3$, 25 °C): δ = 30.0 (d, $^1J_{(Rh,P)}$ = 143.0 Hz, *P*Ph$_3$); IR (KBr): $\tilde{\nu}$ = 3060, 2957, 2926, 2870, 1664, 1533, 1436, 1368, 1260, 1095 cm^{-1}; MS (ESI): *m*/*z* (%): 880.1 [M − Cl]$^+$, 618.2 [M − PPh_3 − Cl]$^+$; elemental analysis calcd. (%) for $C_{46}H_{53}Cl_2N_3O_4PRh$: C 60.27, H 5.83, N 4.58; found: C60.22, H 6.10, N 4.37. Crystal data: formula: $C_{46}H_{53}Cl_2N_3O_4P_1Rh_1$; M_r = 916.69; crystal color and shape: red plate, crystal dimensions: 0.1 × 0.1 × 0.05 mm; crystal system: monoclinic; space group: $P2_1$ (no. 4); a = 8.7620(3), b = 32.5384(10), c = 8.8665(3) Å, α = 90.00°, β = 109.700(2)°, γ = 90.00°; V = 2379.90(14) Å^3; Z = 2; $\mu(Mo_{K\alpha})$ = 0.547 cm^{-1}; ρ_{calcd} = 1.279 g cm^{-3}; θ-range = 2.74–27.65°; data collected: 10,172; independent data [$I_o > 2\sigma(I_o)$/all data/R_{int}]: 9986/10,172/0.039; data/restraints/parameter: 10,172/43/500; $R1$ [$I_o > 2\sigma(I_o)$/all data]: 0.0470/0.0479; $wR2$ [$I_o > 2\sigma(I_o)$/all data]: 0.1214/0.1218; GOF = 1.236; $\Delta\rho_{max/min}$: 0.50/−1.27 e Å^{-3}.

4.2.5.2. [(η^6-C$_6$H$_5$CH$_2$NHCO-Eps-Leu-Bz)RuCl$_2$(PPh$_3$)] ***12***. This compound was synthesized following general procedure A. The product was obtained as a bright red solid (118 mg, 0.14 mmol, 79%). ^{1}H NMR (400 MHz, $CDCl_3$, 25 °C): δ = 7.97 (t, $^3J_{(H,H)}$ = 5.4 Hz, 1H, N*H*CH$_2$), 7.76–7.65 (m, 6H, C$H_{aromat.}$), 7.51–7.22 (m, 14H, C$H_{aromat.}$), 6.76 (d, $^3J_{(H,H)}$ = 8.3 Hz, 1H, N*H*CH), 6.50 (t, $^3J_{(H,H)}$ = 5.4 Hz, 1H, N*H*CH$_2$), 5.61 (d, $^3J_{(H,H)}$ = 5.6 Hz, 1H, CH_{ortho}), 5.35–5.31 (m, 1H, CH_{meta}), 5.29 (d, $^3J_{(H,H)}$ = 6.1 Hz, 1H, CH_{ortho}), 5.12–5.04 (m, 1H, CH_{meta}), 4.68 (dd, $^2J_{(H,H)}$ = 15.4 Hz, $^3J_{(H,H)}$ = 6.2 Hz, 1H, CH_2), 4.61–4.55 (m, 1H, CH_{para}), 4.52–4.30 (m, 5H, PhCH_2/CH_2/CH_2Ph),3.93 (s, 1H, C*H*(O)CH′), 3.57 (s, 1H, CH(O)C*H*′), 1.73–1.50 (m, 3H, $CH_2CH(CH_3)_2$), 0.89 (d, $^3J_{(H,H)}$ = 6.0 Hz, 6H, $CH_2CH(CH_3)_2$); ^{13}C NMR (101 MHz, $CDCl_3$, 25 °C): δ = 171.4 (*C*ON), 167.1 (*C*ON), 166.3 (*C*ON), 138.2 (s, $C_{aromat.}$), 134.2 (d, $J_{(P,C)}$ = 9.2 Hz, $C_{aromat.}$), 133.0 (d, $J_{(P,C)}$ = 47.7 Hz, $C_{aromat.}$), 130.8 (d, $J_{(P,C)}$ = 2.5 Hz, $C_{aromat.}$), 128.7 ($C_{aromat.}$), 128.4 (d, $J_{(P,C)}$ = 10.1 Hz, $C_{aromat.}$), 127.8 ($C_{aromat.}$), 127.5 ($C_{aromat.}$), 107.6 (d, $^2J_{(P,C)}$ = 6.7 Hz, $C_{aromat.}$), 89.5 ($C_{aromat.}$), 88.0 (d, $^2J_{(P,C)}$ = 6.5 Hz, $C_{aromat.}$), 87.6 ($C_{aromat.}$), 86.2 ($C_{aromat.}$), 82.0 ($C_{aromat.}$), 54.5 (*C*H(O)CH), 54.4 (CH(O)*C*H), 51.9 (*C*HCH$_2$), 43.5 (NHC$H_2C_{aromat.}$), 41.0 (NHC$H_2C_{aromat.}$), 40.6 (CH*C*H2), 24.9 (*C*H(CH$_3$)$_2$), 23.0 (CH(*C*H$_3$)$_2$), 22.1 (CH(*C*H$_3$)$_2$); ^{31}P NMR (162 MHz, $CDCl_3$, 25 °C): δ = 27.8 (s, *P*Ph$_3$); IR (KBr): $\tilde{\nu}$ = 3060, 2956, 2927, 1669, 1526, 1482, 1435, 1243, 1093, 697, 527 cm^{-1}; MS (ESI): *m*/*z* (%): 822.1 [M$^+$ − Cl], 1679.8 [2M$^+$ − Cl], 1415.8 [2M$^+$ − PPh_3 − Cl]; elemental analysis calcd. (%) for $C_{42}H_{44}Cl_2N_3O_4PRu$: C 58.81, H 5.17, N 4.90; found: C58.47, H 5.09, N 4.64.

4.2.5.3. [((R,R)-Pyrphos-NH-Eps-Leu-Bz)PdCl$_2$] · HCl ***13***. The product was synthesized via route B and obtained as a yellow solid (172 mg, 0.18 mmol, 92%). Synthesis via Route A: 89%. ^{1}H NMR (400 MHz, $CDCl_3$, 25 °C): δ = 7.92–7.81 (m, 8H, C$H_{aromat.}$), 7.65 (t, $^3J_{(H,H)}$ = 7.5 Hz, 1H, C$H_{aromat.}$), 7.59–7.43 (m, 10H, C$H_{aromat.}$), 7.24 (dd, $^3J_{(H,H)}$ = 6.7 Hz, 2H, C$H_{aromat.}$), 7.15 (d, $^3J_{(H,H)}$ = 7.0 Hz, 1H, C$H_{aromat.}$), 6.97 (d, $^3J_{(H,H)}$ = 7.1 Hz, 1H, CON*H*CH), 6.49 (t, $^3J_{(H,H)}$ = 5.1 Hz, 1H, CON*H*CH$_2$), 4.39–4.35 (m, 1H, NHC*H*CO), 4.34–4.21 (m, 2H, NHCH_2), 3.96 (t, $^3J_{(H,H)}$ = 7.7 Hz, 1H, CHCH_2N), 3.77 (t, $^3J_{(H,H)}$ = 7.7 Hz, 1H, CHCH_2N), 3.52–3.48 (m, 1H, C*H*CH$_2$N), 3.46 (s, 1H, C*H*CH), 3.40 (s, 1H, CHC*H*), 3.25–3.13 (m, 2H, CHCH_2N), 2.92 (t, $^3J_{(H,H)}$ = 8.1 Hz, 1H, C*H*CH$_2$N), 1.61–1.50 (m, 3H, CHCH_2CH), 0.88 (d, $^3J_{(H,H)}$ = 5.4 Hz, 6H, CH(CH_3)$_2$); ^{13}C NMR (101 MHz, $CDCl_3$, 25 °C): δ = 171.3 (CH*C*ONH), 166.0 (NCOCH), 164.0 (CH*C*ONH), 137.6 ($C_{aromat.}$), 136.4 (dd, $^1J_{(P,C)}$ = 13.0 Hz, $C_{aromat.}$), 133.5 (d, $^2J_{(P,C)}$ = 21.1 Hz, $C_{aromat.}$), 133.1 (d, $^2J_{(P,C)}$ = 9.1 Hz, $C_{aromat.}$), 132.6 ($C_{aromat.}$), 129.3 (dt, $^3J_{(P,C)}$ = 8.6 Hz, $C_{aromat.}$), 128.6 ($C_{aromat.}$), 127.5 ($C_{aromat.}$), 127.4 ($C_{aromat.}$), 126.7 (dd, $J_{(P,C)}$ = 17.1 Hz, $C_{aromat.}$), 123.8 ($C_{aromat.}$), 123.2 ($C_{aromat.}$), 53.5 (*C*HCH), 52.8 (CH*C*H), 51.8 (NH*C*HCO), 45.3 (m, *C*HCH$_2$N), 44.0 (m, $^2J_{(P,C)}$ = 15.0 Hz, CHCH_2N), 43.5 (NHCH_2), 43.1 (m, CHCH_2N), 41.2 (CHCH_2CH), 24.8 (*C*H(CH$_3$)$_2$), 22.7 (CH(*C*H$_3$)$_2$), 22.1 (CH(*C*H$_3$)$_2$); ^{31}P NMR (162 MHz, $CDCl_3$, 25 °C): δ = 39.6 (dd, $^2J_{(P,P)}$ = 157.7 Hz, $^3J_{(P,P)}$ = 15.8 Hz, *P*Ph$_2$); IR (nujol): $\tilde{\nu}$ = 1660, 1530 cm^{-1}; HRMS (ESI): *m*/*z*: mass calcd. 897.18434 [M − Cl]$^+$, found: 897.17936 [M − Cl]$^+$, mass calcd.: 956.15079 [M + Na]$^+$, found: 956.13679 [M + Na]$^+$; elemental analysis calcd. (%) for $C_{45}H_{47}Cl_2N_3O_4P_2Pd$ · HCl: C 55.74, H 4.99, N 4.33; found: C 56.30, H 5.02, N 4.53.

4.2.5.4. [((R,R)-Pyrphos-NHCO-Eps-Leu-Bz)PtCl$_2$] ***14***. This compound was synthesized following general procedure B. The product was obtained as a yellow solid (194 mg, 0.19 mmol, 95%). Synthesis via Route A: 87%. ^{1}H NMR (400 MHz, $CDCl_3$, 25 °C): δ = 7.99–7.73 (m, 8H, C*H*$_{aromat.}$), 7.67–7.51 (m, 13H, C*H*$_{aromat.}$), 7.30 (dd, $^3J_{(H,H)}$ = 6.8 Hz, 2H, C*H*$_{aromat.}$), 7.19 (d, $^3J_{(H,H)}$ = 8.2 Hz, 2H, C*H*$_{aromat.}$), 6.64 (d, $^3J_{(H,H)}$ = 8.3 Hz, 1H, CON*H*CH), 6.16 (t, $^3J_{(H,H)}$ = 4.9 Hz, 1H, CON*H*CH$_2$), 4.36–4.28 (m, 3H, NHC*H*CO, NHC*H*$_2$), 4.01 (t, $^3J_{(H,H)}$ = 7.8 Hz, 1H, CHC*H*$_2$N), 3.87 (m, 1H, CHC*H*$_2$N), 3.59 (d, $^3J_{(H,H)}$ = 1.7 Hz, 1H, C*H*CH), 3.40 (d, $^3J_{(H,H)}$ = 1.7 Hz, 1H, CHC*H*), 3.37–3.32 (m, 1H, C*H*CH$_2$N), 3.17–3.11 (m, 1H, CHC*H*$_2$N), 3.08–2.98 (m, 1H, C*H*CH$_2$N), 2.90 (dd, $^3J_{(H,H)}$ = 8.5 Hz, 1H, CHC*H*$_2$N), 1.59–1.48 (m, 3H, CHC*H*$_2$C*H*), 0.80 (d, $^3J_{(H,H)}$ = 5.8 Hz, 6H, CH(C*H*$_3$)$_2$); ^{13}C NMR (101 MHz, $CDCl_3$, 25 °C): δ = 171.1 (CH*C*ONH), 166.1 (N*C*OCH), 164.3 (CH*C*ONH), 137.8 (*C*$_{aromat.}$), 136.5 (m, $^1J_{(P,C)}$ = 11.5 Hz, *C*$_{aromat.}$), 133.4 (d, $^2J_{(P,C)}$ = 20.1 Hz, *C*$_{aromat.}$), 133.1 (m, *C*$_{aromat.}$), 132.4 (*C*$_{aromat.}$), 129.4 (dt, $^3J_{(P,C)}$ = 12.6 Hz, *C*$_{aromat.}$), 128.7 (*C*$_{aromat.}$), 127.6 (*C*$_{aromat.}$), 127.5 (*C*$_{aromat.}$), 125.7 (dd, $J_{(P,C)}$ = 15.3 Hz, *C*$_{aromat.}$), 122.8 (s. *C*$_{aromat.}$), 122.6 (*C*$_{aromat.}$), 53.5 (*C*HCH), 53.0 (CH*C*H), 51.9 (NH*C*HCO), 45.4 (m, *C*HCH$_2$N), 43.9 (m, $^2J_{(P,C)}$ = 15.4 Hz, CHCH$_2$N), 43.5 (NH*C*H$_2$), 42.9 (m, *C*HCH$_2$N), 41.2 (CH*C*H$_2$CH), 24.8 (*C*H(CH$_3$)$_2$), 22.8 (CH(*C*H$_3$)$_2$), 22.1 (CH(*C*H$_3$)$_2$); ^{31}P NMR (162 MHz, $CDCl_3$, 25 °C): δ = 17.9 (ddd, $^2J_{(P,P)}$ = 173.5 Hz, $^3J_{(P,P)}$ = 10.3 Hz, $^1J_{(Pt,P)}$ = 1.66 kHz, *P*Ph$_2$); IR (nujol): $\tilde{\nu}$ = 1662, 1531 cm^{-1}; HRMS (ESI): *m*/*z*: mass calcd. 1027.27218 [M − Cl + CH_3CN]$^+$, found: 1027.26556 [M − Cl + CH_3CN]$^+$; elemental analysis calcd. (%) for $C_{45}H_{47}Cl_2N_3O_4P_2Pt$: C 52.89, H 4.64, N 4.11; found: C 52.86, H 4.62, N 4.10.

4.2.5.5. [(η^5-Me$_4$Cp(CH$_2$)$_2$NHCO-(CH$_2$)$_2$-CONH-(CHPh)-OP(OPh)$_2$)RhCl$_2$PPh$_3$] ***15***. This compound was synthesized following general procedure A. The product was obtained as a bright red solid (139 mg, 0.14 mmol, 68%). ^{1}H NMR (400 MHz, $CDCl_3$, 25 °C): δ = 8.23 (d, $^3J_{(H,H)}$ = 10.0 Hz, 1H, CH$_2$N*H*), 8.07–7.04 (m, 28H, C*H*$_{aromat.}$), 7.00 (t, $^3J_{(H,H)}$ = 5.6 Hz, 1H, NHC*H*), 6.84 (d, $^3J_{(H,H)}$ = 8.0 Hz, 2H, C*H*$_{aromat.}$), 5.90 (dd, $^2J_{(P,H)}$ = 22.2 Hz, $^3J_{(H,H)}$ = 9.7 Hz, 1H, C*H*), 3.48–3.30 (m, 2H, C*H*$_2$NH), 2.48–2.26 (m, 4H, COC*H*$_2$C*H*$_2$), 2.25–2.16 (m, 2H, C*H*$_{2Cp}$), 1.46 (dd, $^3J_{(Rh,H)}$ = 5.6 Hz, $^4J_{(P,H)}$ = 2.4 Hz, 6H, C$_{Cp}$C*H*$_3$), 1.07 (dd, $^3J_{(Rh,H)}$ = 4.2 Hz, $^4J_{(P,H)}$ = 4.2 Hz, 6H, C$_{Cp}$C*H*$_3$); ^{13}C NMR (101 MHz, $CDCl_3$, 25 °C): δ = 172.6 (*C*ON), 172.0 (d, $^4J_{(Rh,C)}$ = 7.7 Hz, *C*O), 150.6 (d, $^3J_{(P,C)}$ = 9.9 Hz, *C*$_{aromat.}$), 150.2 (d, $^4J_{(P,C)}$ = 9.2 Hz, *C*$_{aromat.}$), 134.8 (d, $^3J_{(P,C)}$ = 9.9 Hz, *C*$_{aromat.}$), 134.2 (*C*$_{aromat.}$), 130.6 (*C*$_{aromat.}$), 129.7 (d, $J_{(P,C)}$ = 11.1 Hz, *C*$_{aromat.}$), 128.8 (*C*$_{aromat.}$), 128.5 (d, $J_{(P,C)}$ = 6.1 Hz, *C*$_{aromat.}$), 128.1 (*C*$_{aromat.}$), 125.3 (d, $J_{(P,C)}$ = 4.6 Hz, *C*$_{aromat.}$), 120.6 (d, $J_{(P,C)}$ = 3.9 Hz, *C*$_{Cp}$), 120.5 (d, $J_{(P,C)}$ = 4.2 Hz, *C*$_{aromat.}$), 102.5 (dd, $^1J_{(Rh,C)}$ = 6.9 Hz, $^3J_{(P,C)}$ = 6.9 Hz, *C*$_{Cp}$), 100.5 (dd, $^1J_{(Rh,C)}$ = 6.9 Hz, $^3J_{(P,C)}$ = 6.9 Hz, *C*$_{Cp}$), 96.8 (d, $^1J_{(Rh,C)}$ = 6.9 Hz, *C*$_{Cp}$), 96.6 (d, $^1J_{(Rh,C)}$ = 6.1 Hz, *C*$_{Cp}$), 50.8 (d, $^1J_{(P,C)}$ = 156.4 Hz, *C*H), 36.3 (d, $^4J_{(P,C)}$ = 4.6 Hz, *C*H$_{2Cp}$), 31.8 (s, COC*H*$_2$CH$_2$), 31.5 (s, COCH$_2$*C*H$_2$), 24.7 (s, NHCH$_2$), 9.5 (s, C$_{aromat.}$*C*H$_3$), 8.7 (s, C$_{aromat.}$C*H*$_3$); ^{31}P NMR (162 MHz, $CDCl_3$, 25 °C): δ = 29.9 (d, $^1J_{(Rh,P)}$ = 143.0 Hz, *P*Ph$_3$), 14.8 (s, O*P*(OPh)$_2$); IR (KBr): $\tilde{\nu}$ = 3295, 3057, 2920, 2360, 2225, 1670, 1589, 1522, 1489, 1435, 1384, 1266, 1186, 1161, 1095, 1025 cm^{-1}; MS (ESI): *m*/*z* (%):687.1 [M − PPh$_3$ − 2Cl − H]$^+$, 723.1 [M − PPh$_3$ − Cl]$^+$, 949.1 [2M − 2Cl − H]$^+$, 984.8 [2M − Cl]$^+$; elemental analysis calcd. (%) for $C_{52}H_{53}Cl_2N_2O_5PRh$: C 61.13, H 5.23, N 2.74; found: C 60.18, H 5.51, N 3.00.

4.2.5.6. [(PNP-NCO-(CH$_2$)$_2$-CONH-(CHPh)-OP(OPh)$_2$)PdCl$_2$] · HCl ***16***. This compound was synthesized following general procedure B. The product was obtained as a yellow solid (161 mg, 0.18 mmol, 89%). ^{1}H NMR (400 MHz, $CDCl_3$, 25 °C): δ = 7.67 (1H, m, CON*H*), 7.48 (2H, d, $^3J_{(H,H)}$ = 7.6 Hz, C*H*$_{aromat.}$), 7.31–7.11 (11H, m, C*H*$_{aromat.}$), 6.89 (2H, t, $^3J_{(H,H)}$ = 8.2 Hz, C*H*$_{aromat.}$), 5.88 (1H, dd, $^2J_{(P,H)}$ = 22.0 Hz, $^3J_{(H,H)}$ = 9.6 Hz, N*H*COPO), 3.81–3.64 (4H, m, NC*H*$_2$), 2.69–2.58 (4H, m, C*H*(CH$_3$)$_2$, NCH$_2$C*H*$_2$), 2.28–2.10 (8H, m, COC*H*$_2$C*H*$_2$, C*H*(CH$_3$)$_2$, NCH$_2$C*H*$_2$), 1.21–1.09 (24H, m, CH(C*H*$_3$)$_2$); ^{13}C NMR (101 MHz, $CDCl_3$, 25 °C): δ = 172.1 (d, $^4J_{(P,C)}$ = 7.8 Hz, NCOCH$_2$), 171.9 (*C*ONHCH), 150.5 (d, $^1J_{(P,C)}$ = 9.9 Hz, *C*$_{aromat.}$), 150.1 (d, $^1J_{(P,C)}$ = 9.6 Hz, *C*$_{aromat.}$), 134.3 (*C*$_{aromat.}$), 129.7 (d, $^1J_{(P,C)}$ = 10.5 Hz, *C*$_{aromat.}$), 128.7 (d, $J_{(P,C)}$ = 2.1 Hz, *C*$_{aromat.}$), 128.4 (*C*$_{aromat.}$), 128.3 (*C*$_{aromat.}$), 128.2 (*C*$_{aromat.}$), 125.3 (d, $J_{(P,C)}$ = 5.5 Hz, *C*$_{aromat.}$), 120.7 (d, $J_{(P,C)}$ = 4.2 Hz, *C*$_{aromat.}$), 120.6 (d, $J_{(P,C)}$ = 4.3 Hz, *C*$_{aromat.}$), 51.3 (NCH$_2$), 51.0 (NCH$_2$), 50.6 (d, $^1J_{(P,C)}$ = 157.1 Hz, *C*HP), 31.8 (COCH$_2$CH$_2$CO), 31.5 (COCH$_2$CH$_2$CO), 25.2 (d, $^1J_{(P,C)}$ = 10.0 Hz, PCH(CH$_3$)$_2$), 21.9 (d, $^1J_{(P,C)}$ = 15.7 Hz, NCH$_2$*C*H$_2$), 20.1 (d, $^1J_{(P,C)}$ = 17.2 Hz, NCH$_2$*C*H$_2$), 19.7 (d, $^2J_{(P,C)}$ = 4.8 Hz, CH(*C*H$_3$)$_2$), 19.6 (m, CH(*C*H$_3$)$_2$); ^{31}P NMR (162 MHz, $CDCl_3$, 25 °C): δ = 39.2 (d, $^2J_{(P,P)}$ = 35.6 Hz, *P*^{i}Pr$_2$), 14.5 (s, *P*O(OAr)$_2$); IR (nujol): $\tilde{\nu}$ = 1674, 1640, 1588, 1262, 1210 cm^{-1}; MS (ESI): *m*/*z* (%): 832.3 [M$^+$ − 2Cl], 873.3 [M$^+$ − Cl + CH_3CN]; MS (FAB): *m*/*z* (%): 873.1 [M$^+$ − Cl + CH_3CN]; elemental analysis calcd. (%) for $C_{37}H_{57}Cl_2N_3O_5P_3Pd$ · HCl: C 49.80, H 6.22, N 2.98; found: C 50.25, H 5.98, N 2.71.

4.2.5.7. [(η^5-Me$_4$Cp(CH$_2$)$_2$NHCO-(C$_6$H$_4$)-SO$_2$F)RhCl$_2$(PPh$_3$)] ***17***. This compound was synthesized following general procedure C. The product was obtained as an orange solid (186 mg, 0.24 mmol, 95%). Synthesis via Route A: 59%. ^{1}H NMR (400 MHz, $CDCl_3$, 25 °C): δ = 8.12 (t, $^3J_{(H,H)}$ = 5.8 Hz, 1H, N*H*), 8.03 (d, $^3J_{(H,H)}$ = 8.3 Hz, 2H, C*H*$_{aromat.}$), 7.80–7.72 (m, 8H, C*H*$_{aromat.}$), 7.33–7.14 (m, 9H, C*H*$_{aromat.}$), 3.85 (dt, $^3J_{(H,H)}$ = 5.8 Hz, 2H, CH$_2$C*H*$_2$NH), 2.67 (m, 2H, C*H*$_2$CH$_2$NH), 1.60 (d, 6H, $^4J_{(P,H)}$ = 2.1 Hz, C$_{aromat.}$C*H*$_3$), 0.98 (d, $^4J_{(P,H)}$ = 2.9, 6H, C$_{aromat.}$C*H*$_3$); ^{13}C NMR (101 MHz, $CDCl_3$, 25 °C): δ = 165.0 (*C*ON), 140.2 (*C*$_{aromat.}$), 134.7 (d, $^3J_{(P,C)}$ = 9.2 Hz, *C*$_{aromat.}$), 130.7 (*C*$_{aromat.}$), 129.1 (*C*$_{aromat.}$), 128.4 (*C*$_{aromat.}$), 128.2 (*C*$_{aromat.}$), 103.3 (d, $^2J_{(Rh,C)}$ = 6.2 Hz, *C*$_{aromat.}$), 103.1 (m, *C*$_{aromat.}$), 95.5 (d, $^2J_{(Rh,C)}$ = 7.7 Hz, *C*$_{aromat.}$), 37.1 (d, $^4J_{(P,C)}$ = 4.6 Hz, CH$_2$*C*H$_2$NH), 25.3 (*C*H$_2$CH$_2$NH), 9.8 (C$_{Cp}$*C*H$_3$), 8.6 (C$_{Cp}$*C*H$_3$); ^{31}P NMR (162 MHz, $CDCl_3$, 25 °C): δ = 30.0 (d, $^1J_{(Rh,P)}$ = 143.0 Hz, *P*Ph$_3$); ^{19}F NMR (376 MHz, $CDCl_3$, 25 °C): δ = 85.9 (s, SO$_2$*F*); IR(KBr): $\tilde{\nu}$ = 3056, 2920, 2815, 1664, 1532, 1483, 1435, 1411, 1213, 1095 cm^{-1}. MS (ESI): *m*/*z* (%): 488.0 [M − PPh$_3$ − Cl]$^+$, 749.9 [M − Cl]$^+$; elemental analysis calcd. (%) for $C_{36}H_{36}Cl_2FNO_3PRhS$: C 54.97, H 4.61, N 1.78; found: C 54.48, H 5.29, N 1.84. Crystal data: formula: $C_{75}H_{75}Cl_3F_2N_2O_6P_2Rh_2S_2$; M_r = 1931.12; crystal color and shape: red fragment, crystal dimensions: 0.05 × 0.13 × 0.36 mm; crystal system: triclinic; space group: $P\bar{1}$ (no. 2); a = 15.0745(9), b = 16.9192(10), c = 18.5003(12) Å, α = 69.352(3)°, β = 73.986(4)°, γ = 69.983(3)°; V = 4083.5(4) Å^3; Z = 2; λ(Mo$_{K\alpha}$) = 0.976 mm^{-1}; ρ_{calcd} = 1.571 g cm^{-3}; θ-range = 1.19–25.38°; data collected: 104,799; independent data [$I_o > 2\sigma(I_o)$/all data/R_{int}]: 9487/11,695/0.100; data/restraints/parameter: 11,695/0/945; *R*1 [$I_o > 2\sigma(I_o)$/all data]: 0.0410/0.0574; *wR*2 [$I_o > 2\sigma(I_o)$/all data]: 0.0994/0.1146; GOF = 1.046; $\Delta\rho_{max/min}$: 1.06/−0.77 e Å^{-3}.

4.2.5.8. [(η^6-C$_6$H$_5$CH$_2$NHCO-(C$_6$H$_4$)-SO$_2$F)RuCl$_2$(PPh$_3$)] ***18***. This compound was synthesized following general procedure A. The product was obtained as a bright red solid (63 mg, 0.86 mmol, 43%). ^{1}H NMR (400 MHz, $CDCl_3$, 25 °C): δ = 8.76 (m, 1H, N*H*), 8.26 (d, $^3J_{(H,H)}$ = 8.3 Hz, 2H, C*H*$_{aromat.}$), 7.71–7.26 (m, 6H, C*H*$_{aromat.}$), 7.43–7.37 (m, 9H, C*H*$_{aromat.}$), 5.61 (d, $^3J_{(H,H)}$ = 5.0 Hz, 2H, C*H*$_{aromat.}$), 5.26 (m, 2H, C*H*$_{aromat.}$), 4.75 (d, 2H, $^3J_{(H,H)}$ = 2.5 Hz, NHC*H*$_2$); ^{13}C NMR (101 MHz, $CDCl_3$, 25 °C): δ = 165.4 (*C*ON), 139.9 (*C*$_{aromat.}$), 135.6 (d, $^3J_{(F,C)}$ = 25.4 Hz, *C*$_{aromat.}$), 134.2 (d, $J_{(P,C)}$ = 10.0 Hz, *C*$_{aromat.}$), 132.9 (d, $J_{(P,C)}$ = 47.7 Hz, *C*$_{aromat.}$), 130.9 (d, $J_{(P,C)}$ = 1.5 Hz, *C*$_{aromat.}$), 129.1 (*C*$_{aromat.}$), 128.9 (*C*$_{aromat.}$), 128.4 (d, $J_{(P,C)}$ = 10.0 Hz, *C*$_{aromat.}$), 105.9 (d, $^2J_{(Ru,P)}$ = 7.7 Hz, *C*$_{aromat.}$), 88.8 (d, $^2J_{(Ru,P)}$ = 5.4 Hz, *C*$_{aromat.}$), 87.9 (m, *C*$_{aromat.}$), 82.4 (m, *C*$_{aromat.}$), 41.9 (*C*H$_2$NH); ^{31}P NMR (162 MHz, $CDCl_3$, 25 °C): δ = 28.0 (s, *P*Ph$_3$); ^{19}F NMR (376 MHz, $CDCl_3$, 25 °C): δ = 66.3 (s, SO$_2$*F*); IR (KBr): $\tilde{\nu}$ = 3059, 2920, 2851, 1666, 1528, 1482, 1435, 1412,

1213, 1094, 697 cm^{-1}; MS (ESI): *m/z* (%): 691.9 [M^+ − Cl]; elemental analysis calcd. (%) for $C_{32}H_{27}Cl_2FNO_3PRuS$: C 51.36, H 3.59, N 2.00; found: C 51.98, H 3.88, N 2.03.

4.2.5.9. Fc-CH_2NHCO-(C_6H_4)-SO_2F ***19***. This compound was synthesized following general procedure A. The product was obtained as a yellow solid (17 mg, 0.04 mmol, 20%). ^{1}H NMR (400 MHz, $CDCl_3$, 25 °C): δ = 8.06 (d, $^3J_{(H,H)}$ = 7.7 Hz, 2H, $CH_{aromat.}$), 7.97 (d, $^3J_{(H,H)}$ = 7.7 Hz, 2H, $CH_{aromat.}$), 6.36 (s, 1H, N*H*), 4.35 (s, 2H, CH_2), 4.27 (s, 4H, CH_{Cp}), 4.20 (s, 5H, CH_{Cp}); ^{13}C NMR (101 MHz, $CDCl_3$, 25 °C): δ = 164.6 (*C*ON), 141.2 ($C_{aromat.}$), 135.5 ($C_{aromat.}$), 128.2 ($C_{aromat.}$), 84.0 (C_{Cp}), 68.9 (C_{Cp}), 68.7 (C_{Cp}), 40.0 (CH_2NH); ^{19}F NMR (376 MHz, $CDCl_3$, 25 °C): δ = 66.1 (s, SO_2F); MS (ESI): *m/z* (%): 401.2 [M^+ + H].

4.2.5.10. [(η^5-$Me_4Cp(CH_2)_2NHCO$-$(CH_2)_9$-OP(OEt)F)$RhCl_2(PPh_3)$] ***20***. This compound was synthesized following general procedure C. The product was obtained as a bright red solid (189 mg, 0.22 mmol, 86%). ^{1}H NMR (400 MHz, $CDCl_3$, 25 °C): δ = 7.82–7.78 (m, 6H, $CH_{aromat.}$), 7.37–7.16 (m, 9H, $CH_{aromat.}$), 6.40 (t, $^3J_{(H,H)}$ = 5.8 Hz, 1H, CH_2N*H*), 4.23 (m, 2H, OCH_2CH_3), 3.85 (dt, $^3J_{(H,H)}$ = 6.2 Hz, 2H, CH_2CH_2NH), 2.24 (m, 2H, CH_2CH_2NH), 2.12 (t, $^3J_{(H,H)}$ = 7.9 Hz, 2H, COCH_2CH_2), 1.90–1.81 (m, 4H, CH_2CH_2P), 1.68–1.59 (m, 4H, CH_2CH_2P), 1.56–1.52 (m, 2H, $COCH_2CH_2$), 1.52 (d, 6H, $^4J_{(P,H)}$ = 1.7 Hz, $C_{Cp}CH_3$), 1.36 (t, 3H, $^3J_{(H,H)}$ = 7.1 Hz, $POCH_2CH_3$), 1.25 (m, 10H, $(CH_2)_2(CH_2)_5(CH_2)_2$), 1.11 (d, $^4J_{(P,H)}$ = 2.9, 6H, $C_{Cp}CH_3$); ^{13}C NMR (101 MHz, $CDCl_3$, 25 °C): δ = 173.5 (*C*ON), 134.8 (d, $^3J_{(P,C)}$ = 9.2 Hz, $C_{aromat.}$), 130.6 ($C_{aromat.}$), 128.1 ($C_{aromat.}$), 102.7 (d, $^2J_{(Rh,C)}$ = 6.9 Hz, $C_{aromat.}$), 100.3 (dd, $^2J_{(Rh,C)}$ = 6.9 Hz, $^3J_{(P,C)}$ = 6.9 Hz, $C_{aromat.}$), 96.6 (dd, $^2J_{(Rh,C)}$ = 6.2 Hz, $C_{aromat.}$), 63.1 (d, $^2J_{(P,C)}$ = 7.6 Hz, OCH_2), 36.6 (d, $^4J_{(P,C)}$ = 5.4 Hz, CH_2CH_2NH), 36.3 (d, $^4J_{(P,C)}$ = 5.4 Hz, CH_2CH_2NH), 30.3 (d, $^3J_{(H,H)}$ = 16.9 Hz, 2H, CH_2), 29.3 (d, $^3J_{(H,H)}$ = 3.1 Hz, 2H, CH_2), 29.0 (d, $^3J_{(H,H)}$ = 17.7 Hz, 2H, CH_2), 25.6 (d, $^3J_{(H,H)}$ = 22.3 Hz, 2H, CH_2), 25.2 (d, $^3J_{(H,H)}$ = 22.3 Hz, 2H, CH_2), 25.0 (d, $^3J_{(H,H)}$ = 22.3 Hz, 2H, CH_2), 24.9 (d, $^3J_{(H,H)}$ = 22.3 Hz, 2H, CH_2), 23.7 (d, $^3J_{(H,H)}$ = 22.3 Hz, 2H, CH_2), 21.9 (d, $^3J_{(H,H)}$ = 5.4 Hz, 2H, CH_2), 16.4 (d, $J_{(P,C)}$ = 5.4 Hz, OCH_2CH_3), 9.5 ($C_{Cp}CH_3$), 8.6 ($C_{Cp}CH_3$); ^{31}P NMR (162 MHz, $CDCl_3$, 25 °C): δ = 32.5 (d, $^2J_{(P,F)}$ = 1.07 kHz, OP(OEt)F), 29.8 ($^1J_{(Rh,P)}$ = 142.0 Hz, PPh_3); ^{19}F NMR (376 MHz, $CDCl_3$, 25 °C): δ = −64.6 (d, $^3J_{(P,F)}$ = 1.07 kHz, OP(OEt)*F*); IR (KBr): $\tilde{\nu}$ = 2922, 2851, 1645, 1435, 1384, 1262, 1095, 1035 cm^{-1}. MS (ESI): *m/z* (%): 566.1 [M − PPh_3 − Cl]$^+$, 530.2 [M − PPh_3 − HCl − Cl]$^+$, 792.1 [M − Cl − HCl]$^+$, 827.9 [M − Cl]$^+$; elemental analysis calcd. (%) for $C_{41}H_{57}Cl_2FNO_4P_2Rh$: C 55.79, H 6.51, N 1.59; found: C 55.37, H 6.51, N 1.56.

Acknowledgments

The authors thank Ramona Lex for help with crystallization. This work was supported by KAUST-GCR (FIC/2010/07) and the KAUST baseline fund (J.E.). We also thank the Elitenetzwerk Bayern for graduate fellowships for T.R. and A.N.M.

Appendix A. Supplementary material

CCDC 868620 and 929468 contain the supplementary crystallographic data for this paper. These data can be obtained free of charge from The Cambridge Crystallographic Data Centre via www.ccdc.cam.ac.uk/data_request/cif.

References

[1] (a) Y. Lu, N. Yeung, N. Sieracki, N.M. Marshall, Nature 460 (2009) 855–862;
(b) K. Severin, R. Bergs, W. Beck, Angew. Chem. Int. Ed. 37 (1998) 1634–1654;
(c) R. Razeghifard, B.B., Wallace, R.J. Pace, T. Wydrzynski, Curr. Protein Pept. Sci. 8 (2007) 3–18;
(d) R.H. Holm, P. Kennepohl, E.I. Solomon, Chem. Rev. 96 (1996) 2239–2314.
[2] (a) E. Meggers, Angew. Chem. Int. Ed. 50 (2011) 2442–2448;
(b) S. Fricker, Metallomics 2 (2010) 366;
(c) G. Gasser, I. Ott, N. Metzler-Nolte, J. Med. Chem. 54 (2011) 3–25.
[3] (a) J.K. Willmann, N. Van Bruggen, L.M. Dinkelborg, S.S. Gambhir, Nat. Rev. Drug Discov. 7 (2008) 591–607;
(b) P. Caravan, Acc. Chem. Res. 42 (2009) 851–862;
(c) A. Razgulin, N. Ma, J. Rao, Chem. Soc. Rev. 40 (2011) 4186–4216;
(d) B.M. Zeglis, J.S. Lewis, Dalton Trans. 40 (2011) 6168–6195;
(e) G. Gasser, A.M. Sosniak, M. Metzler-Nolte, Dalton Trans. 40 (2011) 7061–7076;
(f) F.L. Throp-Greenwood, R.G. Balasingham, M.P. Voogan, J. Organomet. Chem. 714 (2012) 12–21;
(g) G. Gasser, A. Pinto, S. Neumann, A.M. Sosniak, M. Seitz, K. Merz, R. Heumann, N. Metzler-Nolte, Dalton Trans. 41 (2012) 2304–2313.
[4] (a) X. Michalet, F.F. Pinaud, L.A. Bentolila, J.M. Tsay, S. Doose, J.J. Li, G. Sundaresan, A.M. Wu, S.S. Gambhir, S. Weiss, Science 307 (2005) 538–544;
(b) C.J. Fahrni, Curr. Opin. Chem. Biol. 11 (2007) 121–127.
[5] (a) J. Dempsey, J. Winkler, H. Gray, Chem. Rev. 110 (2010) 7024–7039;
(b) A.N. Zaykov, B.V. Popp, Z.T. Ball, Chem. Eur. J. 16 (2010) 6651–6659.
[6] K. Hanaoka, K. Kikuchi, H. Kojima, Y. Urano, T. Nagano, J. Am. Chem. Soc. 126 (2004) 12470–12476.
[7] (a) Y. Lu, Curr. Opin. Chem. Biol. 9 (2005) 118–126;
(b) M.G. Savelieff, Y. Lu, J. Biol. Inorg. Chem. 15 (2010) 461–483.
[8] (a) S. Martic, M. Labib, P. Shipman, H.-B. Kraatz, Dalton Trans. 40 (2011) 7264–7290;
(b) D. Ge, R. Levicky, Chem. Commun. 46 (2010) 7190–7192.
[9] (a) P.J. Deuss, R. den Heeten, W. Laan, P.C.J. Kamer, Chem. Eur. J. 17 (2011) 4680–4698;
b) R. den Heerten, B.K. Munoz, G. Popa, P.C.J. Kamer, Dalton Trans. 39 (2010) 8477–8483.
[10] M. Wilson, G. Whitesides, J. Am. Chem. Soc. 100 (1978) 306–307.
[11] T.R. Ward, Acc. Chem. Res. 44 (2011) 47–57.
[12] J. Pierron, C. Malan, M. Creus, J. Gradinaru, I. Hafner, A. Ivanova, A. Sardo, T.R. Ward, Angew. Chem. Int. Ed. 47 (2008) 701–705.
[13] V. Köhler, J. Mao, T. Heinisch, A. Pordea, A. Sardo, Y.M. Wilson, L. Knörr, M. Creus, J.-C. Prost, T. Schirmer, T.R. Ward, Angew. Chem. Int. Ed. 50 (2011) 10863–10866.
[14] C. Lo, M.R. Ringenberg, D. Gnandt, Y. Wilson, T.R. Ward, Chem. Commun. 47 (2011) 12068–12070.
[15] V. Köhler, Y.M. Wilson, M. Dürrenberger, D. GHislieri, E. Churakova, T. Quinto, L. Knörr, D. Häussinger, F. Hollmann, N.J. Turner, T.R. Ward, Nat. Chem. 5 (2013) 93–99.
[16] T.K. Hyster, L. Knör, T.R. Ward, T. Rovis, Science 338 (2012) 500–503.
[17] (a) P.J. Deuss, G. Popa, C.H. Botting, W. Laan, P.C.J. Kamer, Angew. Chem. Int. Ed. 49 (2010) 5315–5317;
(b) B. Talbi, P. Haquette, A. Martel, F. De Montigny, C. Fosse, S. Cordier, T. Roisnel, G. Jaouen, M. Salmain, Dalton. Trans. 39 (2010) 5605–5607;
(c) M. Reetz, M. Rentzsch, A. Pletsch, M. Maywald, Chimia 56 (2002) 721–723;
(d) L. Panella, J. Broos, J. Jin, M. Fraaije, D. Janssen, M. Jeronimus-Stratingh, B. Feringa, A. Minnaard, J. de Vries, Chem. Commun. (2005) 5656–5658.
[18] (a) C. Kruithof, M. Casado, G. Guillena, M. Egmond, A. van der Kerk-van Hoof, A. Heck, R. Gebbink, G. van Koten, Chem. Eur. J. 11 (2005) 6869–6877;
(b) C.A. Kruithof, H.P. Dijkstra, M. Lutz, A.L. Spek, M.R. Egmond, R.J.M.K. Gebbink, G. Van Koten, Eur. J. Inorg. Chem. (2008) 4425–4432;
(c) H.P. Dijkstra, H. Sprong, B.N.H. Aerts, C.A. Kruithof, M.R. Egmond, R.J.M.K. Gebbink, Org. Biomol. Chem. 6 (2008) 523–531.
[19] (a) M.T. Reetz, M. Rentzsch, A. Pletsch, A. Taglieber, F. Hollmann, R.J.G. Mondière, N. Dickmann, B. Höcker, S. Cerrone, M.C. Haeger, et al., Chem. Biol. Chem. 9 (2008) 552–564;
(b) F. Monnard, T. Heinisch, E. Nogueira, T. Schirmer, T. Ward, Chem. Commun. 47 (2011) 8238–8240;
(c) J. Carey, S. Ma, T. Pfister, D. Garner, H. Kim, J. Abramite, Z. Wang, Z. Guo, Y. Lu, J. Am. Chem. Soc. 126 (2004) 10812–10813;
(d) M. Ohashi, T. Koshiyama, T. Ueno, M. Yanase, H. Fujii, Y. Watanabe, Angew. Chem. Int. Ed. 42 (2003) 1005–1008;
(e) R. Davies, M. Distefano, J. Am. Chem. Soc. 119 (1997) 11643–11652.
[20] T. Reiner, D. Jantke, A.N. Marziale, A. Raba, J. Eppinger, Chem. Open 2 (2013) 50–54.
[21] E.M. Sletten, C.R. Bertozzi, Angew. Chem. Int. Ed. 48 (2009) 6974–6998.
[22] T. Reiner, D. Jantke, A. Raba, A.N. Marziale, J. Eppinger, J. Organomet. Chem. 694 (2009) 1934–1937.
[23] (a) T. Reiner, M. Waibel, A.N. Marziale, D. Jantke, F.J. Kiefer, T.F. Fässler, J. Eppinger, J. Organomet. Chem. 695 (2010) 2667–2672;
(b) T. Reiner, D. Jantke, X.-H. Miao, A.N. Marziale, F.J. Kiefer, J. Eppinger, Dalton Trans. 42 (2013) 8692–8703.
[24] (a) S. Huikai, W. Quingmin, H. Runqiu, L. Heng, L. Yonghong, J. Organomet. Chem. 655 (2002) 182–185;
(b) J. Eppinger, K.R. Nikolaides, M. Zhang-Presse, F.A. Riederer, G.W. Rabe, A.L. Rheingold, Organometallics 27 (2008) 736–740.
[25] (a) A.N. Marziale, E. Herdtweck, J. Eppinger, S. Schneider, Inorg. Chem. 48 (2009) 3699–3709;
(b) T. Hayashi, K. Kanehira, H. Tsuchiya, M. Kumada, J. Chem. Soc. Chem. Commun. (1982) 1162–1164;
(c) T. Hayashi, K. Kanehira, T. Hagihara, M. Kumada, J. Org. Chem. 53 (1988) 113–120.

[26] (a) U. Nagel, J. Leipold, Chem. Ber. 129 (1996) 815–821;
(b) Y. Ribourdouilee, G.D. Engel, M. Richard-Plouet, L.H. Gade, Chem. Commun. (2003) 1228–1229.
[27] (a) B.M. Still, P.G. Anil Kumar, J.R. Aldrich-Wright, W.S. Price, Chem. Soc. Rev. 36 (2007) 668–686;
(b) J.R.L. Piqueler, I.S. Butler, F.D. Rochon, Appl. Spectrosc. Rev. 41 (2006) 185–226.
[28] J.C. Powers, J.L. Asgian, Z.D. Ekici, K.E. James, Chem. Rev. 102 (2002) 4639–4750.
[29] B.J. Gour-Salin, P. Lachance, M.-C. Magny, C. Plouffe, R. Ménard, A.C. Storer, Biochem. J. 299 (1994) 389–392.
[30] Y. Liu, M.P. Patricelli, B.F. Cravatt, Proc. Natl. Acad. Sci. U. S. A. 96 (1999) 14694–14699.
[31] K.A.H. Chehade, A. Baruch, S.H.L. Verhelst, M. Bogyo, Synthesis (2005) 240–244.
[32] V. Tedesco, W. von Philipsborn, Magn. Reson. Chem. 34 (1996) 373–376.
[33] J. Oleksyszyn, L. Subotkowska, P. Mastalerz, Synthesis (1979) 985–986.
[34] Data Collection Software and Data Processing Software for Stoe IPDS 2T Diffractometer, X-ARERA, Version 1.26, Stoe & Cie, Darmstadt, Germany, 2004.
[35] Data Processing Software for Stoe IPDS 2T Diffractometer, XRED, XSHAPE, Version 1.26, Stoe & Cie, Darmstadt, Germany, 2004.
[36] A. Altomare, G. Cascarano, C. Giacovazzo, A. Guagliardi, M.C. Burla, G. Polidori, M. Camalli. SIR92, J. Appl. Cryst. 27 (1994) 435–436.
[37] A.J.C. Wilson (Ed.), International Tables for Crystallography, vol. C, Kluwer Academic Publishers, Dordrecht, The Netherlands, 1992, pp. 193–199. Tables 6.1.1.4 (pp. 500–502), 4.2.6.8 (pp. 219–222), and 4.2.4.2.
[38] G.M. Sheldrick, SHELXL-97, University of Göttingen, Göttingen, Germany, 1998.
[39] A.L. Spek, PLATON, a Multipurpose Crystallographic Tool, Utrecht University, Utrecht, The Netherlands, 2010.
[40] L.J. Farrugia. WinGX (Version 1.70.01 January 2005), J. Appl. Cryst. 32 (1999) 837–838.